

High Step-up Converter for Closed Loop Controller with Three-Winding Coupled Inductor for Renewable Energy Sources

K. Vijay Kumar

Associate Professor, Dept of EEE, Dadi Institute of Engineering and Technology, Anakapalle, Visakhapatnam (Dt), AP, India.

Abstract: Due the increased cost of fuels used for electrical energy generation, present electrical generation units preferred for clean and green type of renewable energy sources. Hence, renewable energy sources such as fuel cells, solar energy, and wind power have been widely valued and employed. Fuel cells have been considered as an excellent candidate to replace the conventional diesel/gasoline in vehicles and emergency power sources. Fuel cells can provide clean energy to users without CO₂ emissions. Due to stable operation with high-efficiency and sustainable/renewable fuel supply, fuel cell has been increasingly accepted as a competently alternative source for the future. The excellent features such as small size and high conversion efficiency make them valuable and potential. Hence, the fuel cell is suitable as power supplies for energy source applications. The generated voltage of the fuel cell stack is rather low. Hence, a high step-up converter is strongly required to lift the voltage for applications such as dc micro grid, inverter, or battery. This concept presents a high step-up converter for fuel cell energy source applications. The proposed high step-up dc-dc converter is devised for boosting the voltage generated from fuel cell to be a 400-V dc-bus voltage. Through the three-winding coupled inductor and voltage doublers circuit, the proposed converter achieve high step-up voltage gain without large duty cycle. This paper proposes a new converter strategy with closed loop control action, with the help of closed loop system attains low steady state error value and system operates in high stability factor for autonomous. Overall performance of the renewable energy system is then affected by the efficiency of step-up DC/DC converters, which are the key parts in the system power chain.

Keywords: Coupled Inductor, Fuel Cell Energy Source Applications, High Step-Up Converter.

I. INTRODUCTION

Renewable energy sources (RES) have experienced a fast development in recent years. These systems employ with micro sources like PV, fuel cells etc. Though PV cells can be made into array and connected in series to produce high voltage there exist serious problems like shadowing effects, short circuit which drastically reduces its efficiency. In order to overcome such adverse effects this micro source energy is

utilized by the high step up converter to produce high voltage and satisfy the demands. Conventional boost converters can't provide such a high DC voltage gain for extreme duty cycle. Thus high step up dc-dc converters are used as front end converters to step from low voltage to high voltage which are required to have a large conversion ratio, high efficiency and small volume [1]. In some converters active clamp circuit is used to overcome voltage spikes caused by the leakage inductance of the coupled inductor. Though ZVS technique is employed for soft switching it can't sustain light loads [2]. Different switching structures are formed either two capacitor or two inductor with two three diodes. Both the step up and step down operations can be performed in this topology, Performance of hybrid converters are better than classical converters but still its costlier to implement [3]. Low level voltage from the PV, fuel cells is connected to Kilo watt level using step up dc-dc converter and inverter circuits. Voltage spikes and switching losses are eliminated by active clamping. In dc-ac, inverter always tends to draw ac ripple current at twice the output frequency. Resonant inductors cost and circuit volume is high [4].

This converter requires a multi winding transformer which makes the circuit design complex [5]. This converter avoids extremely narrow turn off period, ripples and switching losses are eliminated by ZVS technique. It uses two coupled inductors which makes the circuit complex [6]. In this converter no additional magnetic components used, switching losses are minimized by adopting a regenerative snubber circuit. As the circuit uses more switches controlling is complex [7]. In this converter high voltage gain is obtained but the circuit has more passive components [8]. It employees single ended scheme cost is reduced. Galvanic isolation is needed, but suitable only for low power and frequency applications [9], [10]. In this converter no need of extreme duty ratio but if conduction losses or switching losses occurs the efficiency is reduced [11]. It is possible to generate the non-isolated dc-dc converters but the major drawback is that switching frequency must be maintained constant and the turn ratio of the auto transformer must be unity [12]. Some converters operate at very high frequency with fast transient response.

The main switch is fabricated from an integrated power process, the layouts can be changed to vary the parasitic, however design of switch layout is complex, fixed frequency and constant duty ratio must be maintained [13]. This converter provides high voltage gain and can be employed for high power applications however the duty ratio is limited to 0.85. In this, the energy of the leakage inductor is recycled to the output load directly, limiting the voltage spike on the main switch. To achieve a high step-up gain, it has been proposed that the secondary side of the coupled inductor can be used as fly back and forward converters. In some converters voltage gain is improved through output voltage stacking [14].

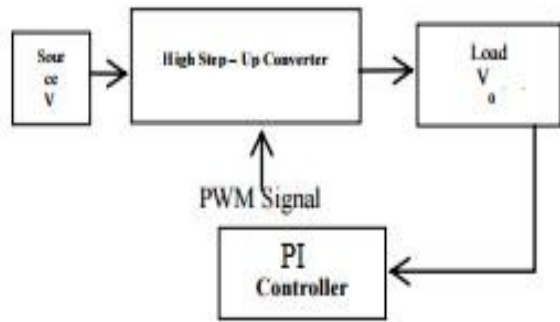


Fig. 1 Block Diagram.

The main objective is to improve the Voltage Gain of the Step-up Converter and also to reduce Voltage stress of the circuit. Further the Voltage Drift problem is reduced using closed loop control of the proposed converter with PI controller. From Fig.1, The output voltage from the converter is fed as feed back to the PI; there it compares the feedback voltage signal and the reference voltage signal to produce PWM pulse which triggers the main switch of the converter.

II. OPERATING PRINCIPLE OF THE PROPOSED CONVERTER

The proposed converter employs a switched capacitor and a voltage-doubler circuit for high step-up conversion ratio. The switched capacitor supplies an extra step-up performance; the voltage-doubler circuit lifts of the output voltage by increasing the turn's ratio of coupled-inductor. The advantages of proposed converter are as follows:

- Through adjusting the turns ratio of coupled inductor, the proposed converter achieves high step-up gain that renewable energy systems require;
- Leakage energy is recycled to the output terminal, which improves the efficiency and alleviates large voltage spikes across the main switch;
- Due to the passive lossless clamped performance, the voltage stress across main switch is substantially lower than the output voltage;
- Low cost and high efficiency are achieved by adopting low-voltage-rated power switch with low RDS-ON;
- By using three-winding coupled inductor, the proposed converter possesses more flexible adjustment of voltage conversion ratio and voltage stress on each diode.

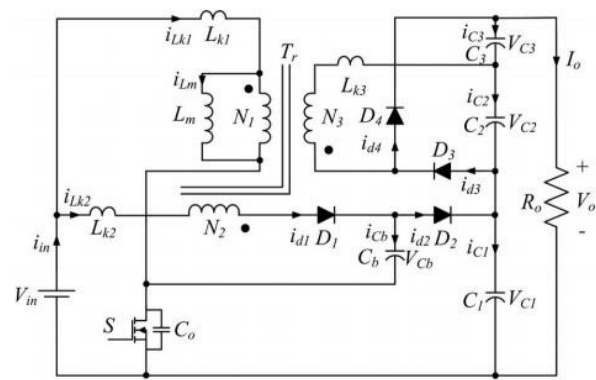


Fig. 2. Equivalent circuit of the proposed converter.

The equivalent circuit of the proposed converter shown in Fig. 2 is composed of a coupled inductor T_r , a main power

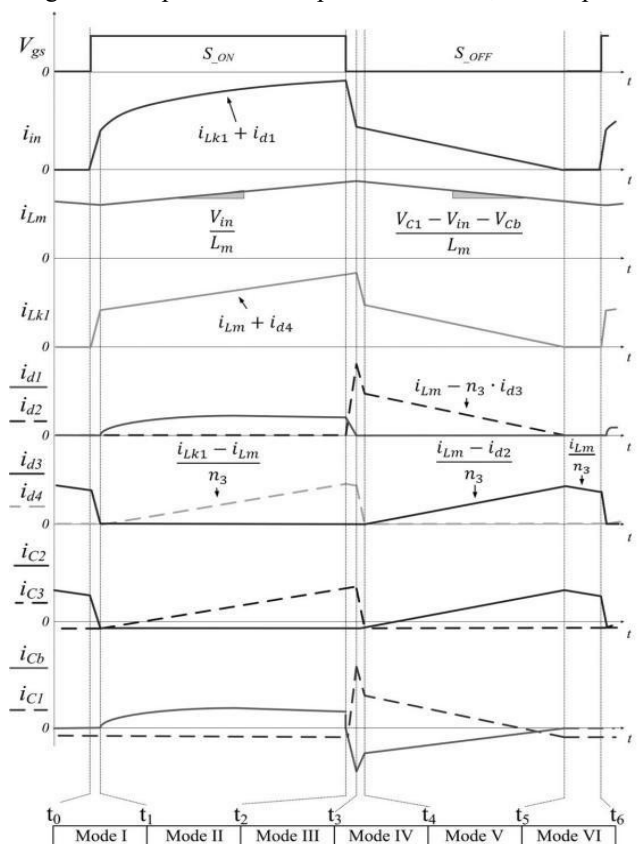


Fig. 3. Steady-state waveforms in CCM operation.

Switch S, diodes D1, D2, D3, and D4, the switched capacitor C_b , and the output filter capacitors $C1$, $C2$, and $C3$. L_m is the magnetizing inductor and L_{k1} , L_{k2} , and L_{k3} represent the leakage inductors. The turn's ratio of coupled inductor n_2 is equal to N_2/N_1 , and n_3 is equal to N_3/N_1 , where N_1 , N_2 , and N_3 are the winding turns of coupled inductor. The steady-state waveforms of the proposed converter operating in CCM are depicted in Fig. 3. The each operating modes is shown in Fig. 4.

Mode I [t_0, t_1]: During this interval, the switch S is turned ON at t_0 . The diodes D1, D2, and D4 are reverse biased. The path of current flow is shown in Fig. 4(a). The primary

High Step-Up Converter for closed loop controller with Three-Winding Coupled Inductor for Renewable Energy Sources

leakage inductor current i_{Lk1} increases linearly, and the energy stored in magnetizing inductance still transfers to the load and output capacitor $C2$ via diode $D3$.

Mode II [t_1, t_2]: During this interval, the switch S is still in the turn-on state. The diodes $D1$ and $D4$ are forward biased; diodes $D2$ and $D3$ are reverse biased. The path of current flow is shown in Fig. 4(b). The dc source V_{in} still charges into the magnetizing inductor L_m and leakage inductor L_{k1} , and the currents through these inductors rise linearly. Some of the energy from dc source V_{in} transfer to the secondary side of the coupled inductor to charge the capacitor $C3$. The switched capacitor C_b is charged by the LC series circuit.

in Fig. 4(d). The current i_{d4} charges the output capacitor $C3$ and decreases linearly. The total voltage of $V_{in} + V_{Lm} + V_C$ is charging to clamped capacitor $C1$, and some of the energy is supplied to the load.

Mode V [t_4, t_5]: During this interval, switch S is still in the turn-off state. The diodes $D1$ and $D4$ are turned OFF; the diodes $D2$ and $D3$ are forward biased. The current-flow path is shown in Fig. 4(e). The energy of the primary side still charges to the clamped capacitor $C1$ and supplies energy to the load. Some of the energy from dc source V_{in} is transferred to the secondary side of the coupled inductor to charge the capacitor $C2$, and the current i_{d3} increases linearly.

Mode VI [t_5, t_6]: During this interval, switch S is still in the turn-off state. The diodes $D1, D2,$ and $D4$ are reverse biased; the diode $D3$ is forward biased. The current-flow path is shown in Fig. 4(f). The current i_{Lk1} is dropped till zero. The magnetizing inductor L_m continuously transfers energy to the third leakage inductor L_{k3} and the capacitor $C2$. The energies are discharged from $C1$ and $C3$ to the load. The current i_{d3} charges $C2$ and supplies the load current.

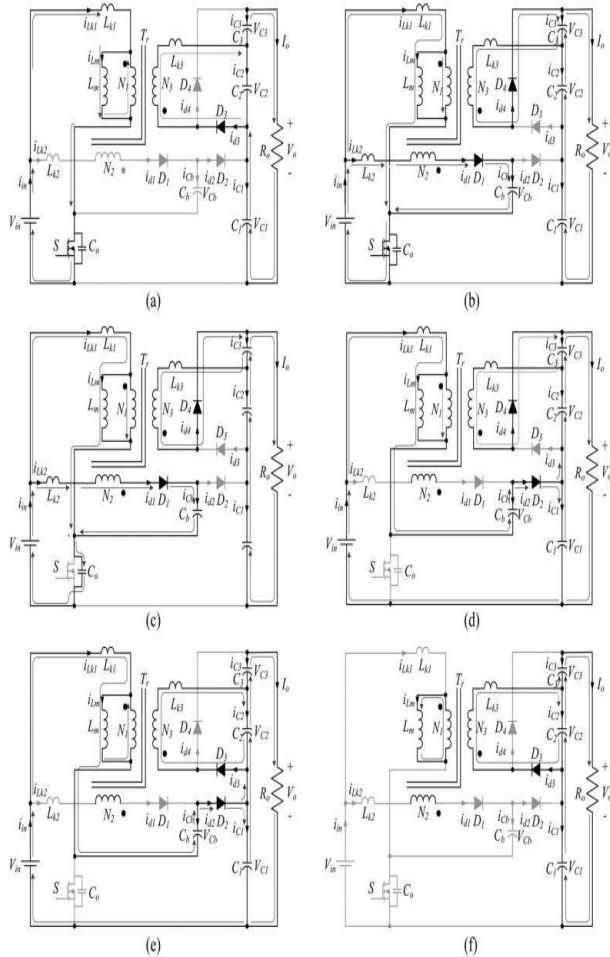


Fig. 4. CCM operating modes of the proposed converter. (a) Mode I [t_0, t_1]. (b) Mode II [t_1, t_2]. (c) Mode III [t_2, t_3]. (d) Mode IV [t_3, t_4]. (e) Mode V [t_4, t_5]. (f) Mode VI [t_5, t_6].

Mode III [t_2, t_3]: During this interval, the switch S is turned OFF at t_2 . Diodes $D1$ and $D4$ are still forward biased; diodes $D2$ and $D3$ are reverse biased. The path of current flow is shown in Fig. 4(c). The magnetizing current and LC series current charge the parasitic capacitor C_o of the MOSFET.

Mode IV [t_3, t_4]: During this interval, S is still in the turnoff state. The diodes $D1, D2,$ and $D4$ are forward biased. The diode $D3$ is reverse biased. The current-flow path is shown

III. STEADY-STATE ANALYSIS

In order to simplify the CCM steady-state analysis, the following factors are taken into account. All the leakage inductors of the coupled inductor are neglected, and all of components are ideal without any parasitic components. The voltages $V_b, V_{C1}, V_{C2},$ and V_{C3} are considered to be constant due to infinitely large capacitances.

A. Step-Up Gain

During the turn-on period of switch S , the following equations can be written as:

$$V_{C3} = V_{N3} = n_3 \cdot V_{in} \tag{1}$$

$$V_{Cb} = V_{in} + V_{N2} = (n_2 + 1) \cdot V_{in} \tag{2}$$

During the turn-off period of switch S , the following equations can be expressed as:

$$V_{C2} = n_3 [V_{C1} - (2 + n_2) \cdot V_{in}] \tag{3}$$

$$V_{C1} = \left(\frac{D}{1 - D} + 2 + n_2 \right) \cdot V_{in} \tag{4}$$

Thus, the output voltage V_O can be expressed as

$$V_O = V_{C1} + V_{C2} + V_{C3} \tag{5}$$

By substituting (1), (3), and (4) into (5), the voltage gain of the proposed converter is given by

$$M_{CCM} = \frac{V_o}{V_{in}} = n_2 + \frac{2 - D + n_3}{1 - D} \tag{6}$$

Equation (6) shows that high step-up gain can be easily obtained by increasing the turn's ratio of the coupled

inductor without large duty cycle. The step-up gain versus duty ratio under various turns' ratios is plotted.

B. Voltage Stress

The voltage stress on the main switch is given as follows:

$$M_S = \frac{V_{S1}}{V_{out}} = \frac{1}{2 - D + (1 - D)n_2 + n_3} \quad (7)$$

When the switching S is turned OFF, the diodes D1 and D3 are reverse biased. Therefore, the voltage stresses of D1 and D3 are as follows:

$$M_{D1} = \frac{V_{D1}}{V_{out}} = \frac{1 + n_2}{2 - D + (1 - D)n_2 + n_3} \quad (8)$$

$$M_{D4} = \frac{V_{D3}}{V_{out}} = \frac{n_3}{2 - D + (1 - D)n_2 + n_3} \quad (9)$$

When the switch S is in turn-on period and the diodes D2 and D3 are reverse biased. Therefore, the voltage stresses of diodes

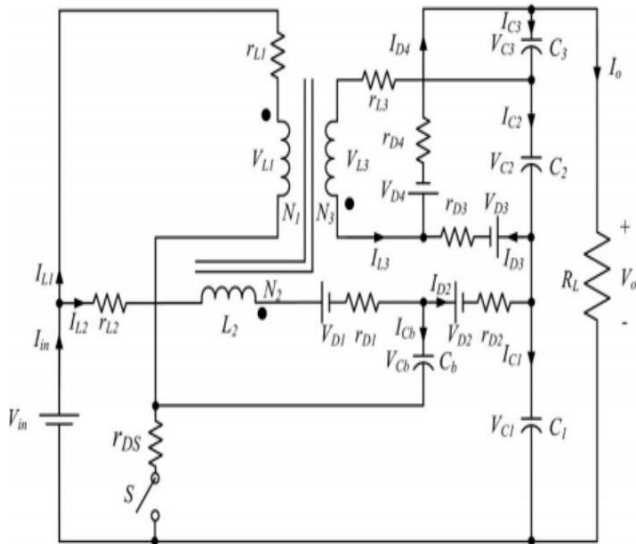


Fig. 5. Equivalent circuit including inductor conduction losses.

D2 and D3 are as follows:

$$M_{D2} = \frac{V_{D2}}{V_{out}} = \frac{1}{2 - D + (1 - D)n_2 + n_3} \quad (10)$$

$$M_{D3} = \frac{V_{D4}}{V_{out}} = \frac{n_3}{2 - D + (1 - D)n_2 + n_3} \quad (11)$$

Equations (7)–(11) can be illustrated to determine the maximum voltage stress on each power drives.

C. Analysis of Conduction Losses

Some conduction losses are caused by resistances of semiconductor components and coupled inductor. Thus, all the components in the analysis of conduction losses are not continuously assumed to be ideal, except for all the capacitors. Diode reverse recovery problems, core losses, switching losses, and the ESR of capacitors are not discussed in this section. The characteristics of leakage inductor are

disregarded because of energy recycling. The equivalent circuit, which includes the conduction losses of coupled inductors and semiconductor components, is shown in Fig.5. The corresponding equivalent circuit includes copper resistances r_{L1} , r_{L2} , and r_{L3} , all the diode forward resistances r_{D1} , r_{D2} , r_{D3} , and r_{D4} , and the on-state resistance R_{DS-ON} of the power switch. Small-ripple approximation was used to calculate conduction losses and all currents that pass through components were approximated by the dc components.

TABLE I: Comparison between Three-Winding Coupled Inductor High Step-Up Converters

Converter Type	$M = \frac{V_{out}}{V_{in}}$	$M_S = \frac{V_{DS}}{V_{out}}$
Proposed converter	$n_2 + \frac{2-D+n_3}{1-D}$	$\frac{1}{1 + (n_2 + n_3) \cdot D + n_2 \cdot (1-D)}$
Converter in [37]	$n_3 + \frac{1 + (n_2 + n_3) \cdot D}{1-D}$	$\frac{1}{1 + n_3 \cdot D + (1 + n_3) \cdot (1+D)}$
Converter in [39]	$(1 + n_2) + \frac{1 + D \cdot n_3}{1-D}$	$\frac{1}{2 - D + n_2 \cdot (1 - D) + n_3}$

Thus, the magnetizing current and capacitor voltages are assumed to be constant. Finally, through voltage–second balance and capacitor-charge balance, the voltage conversion ratio with conduction losses can be derived from

$$\frac{V_o}{V_{in}} = \frac{\left(n_2 + \frac{2-D+n_3}{1-D}\right) - K}{1 + \frac{\alpha}{R_L(1-D)^2} + \frac{r_{L3}}{R_L D(1-D)} + \frac{\beta}{R_L(1-D)} + \frac{\gamma}{R_L D}} \quad (12)$$

Where

Efficiency is expressed as follows:

$$\eta = \frac{V_{in} - n_2 + \frac{2-D+n_3}{1-D} \cdot (V_{D1} + V_{D2} + V_{D3} + V_{D4})}{V_{in} + \frac{\alpha}{R_L(1-D)^2} + \frac{r_{L3}}{R_L D(1-D)} + \frac{\beta}{R_L(1-D)} + \frac{\gamma}{R_L D}} \quad (13)$$

On the basis of (13), it can be inferred that the efficiency will be higher if the input voltage is substantially higher than the summation of the forward bias of all the diodes, or if the load is substantially larger than the resistances of coupled inductors and semiconductor components. In addition, the maximally effect for efficiency is duty cycle, and the secondary is copper resistance of the coupled inductor.

D. Comparison between the Proposed Converter and the Other High Step-Up Converters

The performance of the proposed converter is verified by an analytical comparison with other three-winding coupled inductor high step-up converters for fuel cell, and it is assumed that all the converters are operated in CCM. Moreover, for the sake of fair comparison, the analysis will

High Step-Up Converter for Closed loop controller with Three-Winding Coupled Inductor for Renewable Energy Sources

also assume that the input voltage and the turn's ratios of coupled inductor are the same: $n_2 = 1.5$; $n_3 = 1.5$. Table I summarizes the voltage conversion ratio and the switch stress for the proposed converter and the other single switch high step-up converter topologies introduced. In this comparison between the proposed converter and other converter, n_2 is defined as the turn's ratio N_2/N_1 ; and n_3 is defined as the turn's ratio N_3/N_1 .

IV. MATLAB/SIMULATION RESULTS

Simulation results of this paper is as shown in bellow Figs.6 to 14.

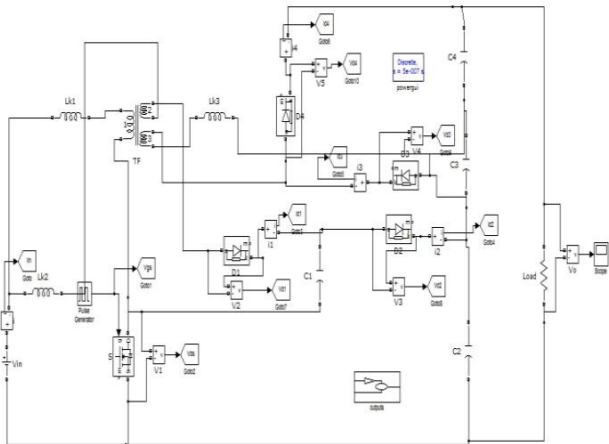


Fig.6. Matlab/simulation model of high step up Converter.

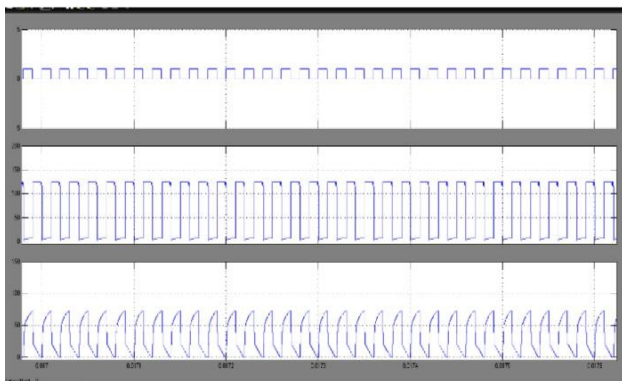


Fig.7. Simulation waveform of gate voltage (Vgs), diode Voltage (Vds), Input Current (iin).



Fig.8. Simulation waveform of diode voltage (Vds), diode Current (Id1), diode Current (id2).

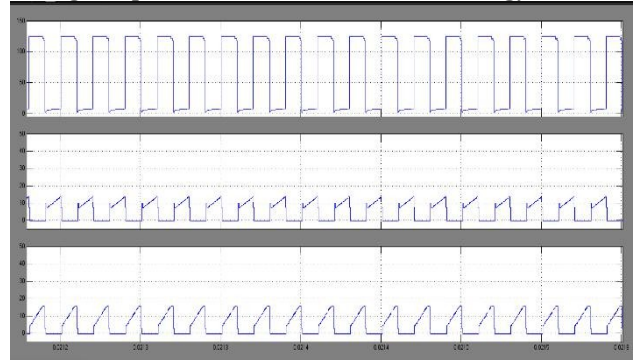


Fig.9. Simulation waveform of diode voltage (Vds), diode Current (Id4), diode Current (id3).

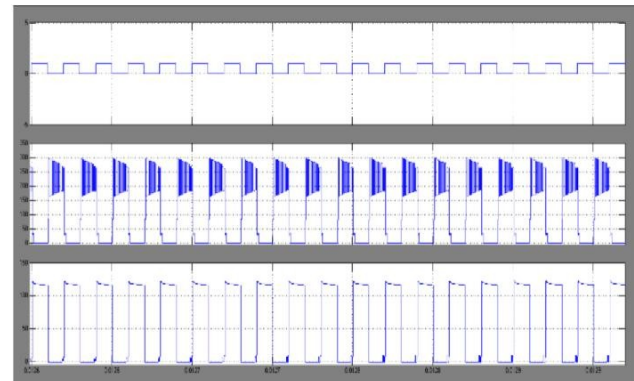


Fig.10. Simulation waveform of gate voltage (Vgs), diode Voltage (Vd2), diode Voltage (Vd2).

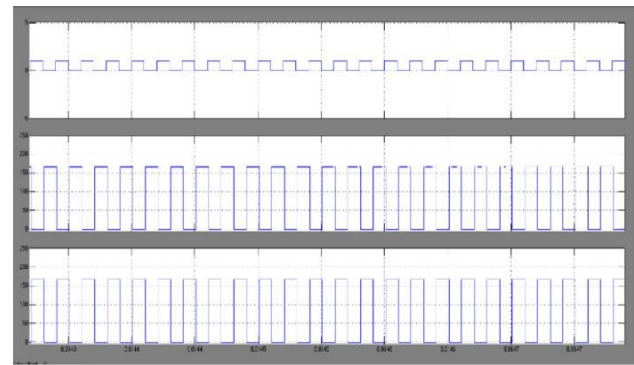


Fig.11. Simulation waveform of gate voltage (Vgs), diode Voltage (Vd4), diode Voltage (Vd3).

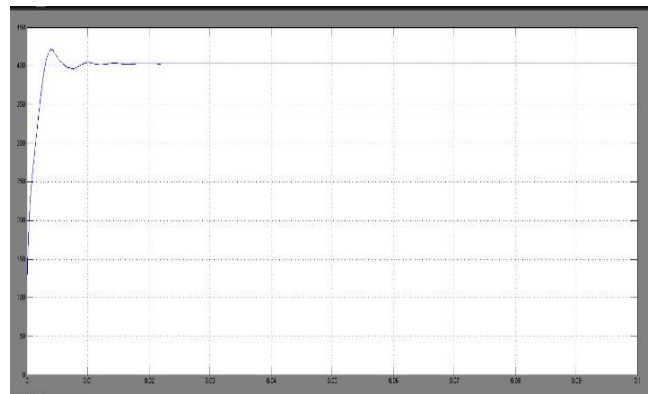


Fig.12. output Voltage of high step up Converter.

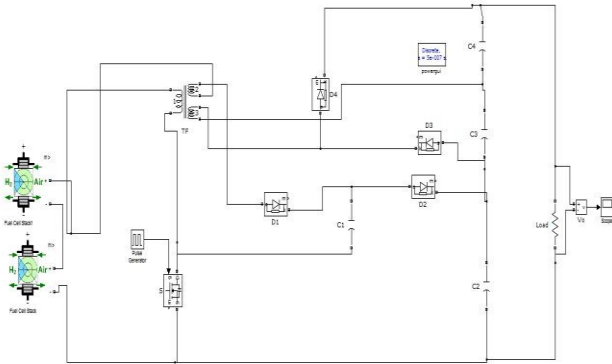


Fig.13.Matlab/Simulation model of high step up Converter with fuel cell.

Fig.16. shows the Converter Output Voltage of Proposed Converter Operating under Closed Loop System compare to open loop system, here attain fast response because of low steady state error value and system may operate under good stability factor.

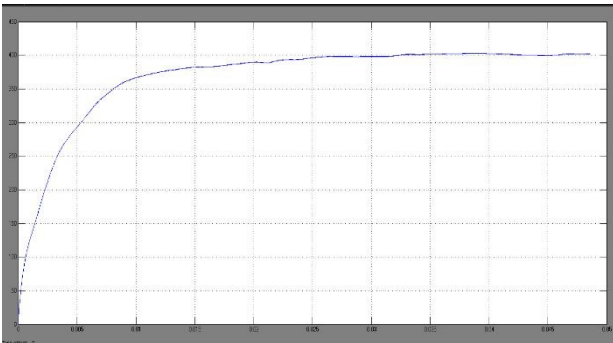


Fig.14.output Voltage of high step up Converter with fuel cell.

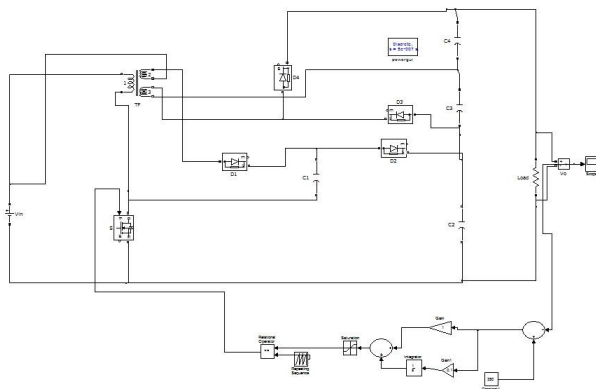


Fig.15.Matlab/simulation model of Closed loop Control of high step up Converter.

Fig.15. shows the Matlab/Simulink Model of Proposed Converter Operating under Closed Loop System using Matlab/Simulink platform.

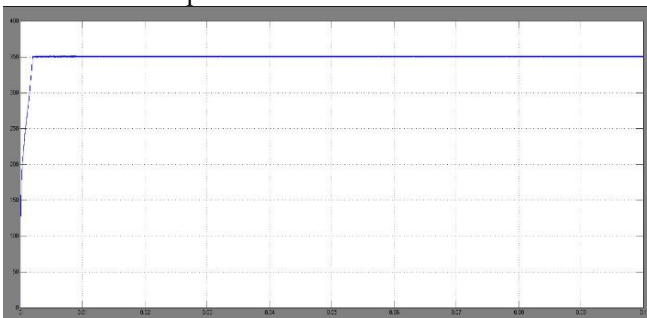


Fig.16.Output Voltage of high step up Converter with closed loop Controller.

V. CONCLUSION

Since DC power sources are widely used in many applications like DC power supplies, battery chargers, and

lighting systems .The high step up dc–dc converters are usually used as the front-end converters to step-up from low voltage to high voltage which are required to have a

large conversion ratio, high efficiency, and small volume. This proposed converter combines a quadratic boost converter with coupled inductor and diode-capacitor techniques for attaining high voltage values. A clamped-capacitor circuit is connected to the primary side of the coupled inductor, the voltage stress of the active switch is reduced greatly and the clamped capacitor also transfers the primary leakage energy to the output. At last a same converter applied to DC bus system and is controlled by closed loop PI control strategy with good dynamic response and low steady state error value with high stability factor.

VI. REFERENCES

- [1] Kuo-Ching Tseng, Jang-Ting Lin, and Chi-Chih Huang” High Step-Up Converter with Three-Winding Coupled Inductor for Fuel Cell Energy Source Applications” IEEE Transactions On Power Electronics, Vol. 30, No. 2, February 2015.
- [2] W. Li, X. Lv, Y. Deng, J. Liu, and X. He, “A review of non-isolated high step-up DC/DC converters in renewable energy applications,” in Proc. IEEE Appl. Power Electron. Conf. Expo., Feb. 2009, pp. 364–369.
- [3] W. Li and X. He, “Review of non-isolated high-step-up DC/DC converters in photovoltaic grid-connected applications,” IEEE Trans. Ind. Electron., vol. 58, no. 4, pp. 1239–1250, Apr. 2011.
- [4] M. A. Laughton, “Fuel cells,” IEE Eng. Sci. Edu. J., vol. 11, no. 1, pp. 7–16, Feb. 2002.
- [5] W. Jiang and B. Fahimi, “Active current sharing and source management in fuel cell-battery hybrid power system,” IEEE Trans. Ind. Electron., vol. 57, no. 2, pp. 752–761, Feb. 2010.
- [6] P. Thounthong, S. Rael, and B. Davat, “Analysis of super capacitor as second source based on fuel cell power generation,” IEEE Trans. Ind. Electron., vol. 24, no. 1, pp. 247–255, Mar. 2009.
- [7] A. Khaligh and Z. Li, “Battery, ultra capacitor, fuel cell, and hybrid energy storage systems for electric, hybrid electric, fuel cell, and plug-in energy source applications: State of the art,” IEEE Trans. Veh. Technol., vol. 59, no. 6, pp. 2806–2814, Jul. 2010.
- [8] L. Wang and H. Li, “Maximum fuel economy-oriented power management design for a fuel cell vehicle using battery and ultra-capacitor,” IEEE Trans. Ind. Appl., vol. 46, no. 3, pp. 1011–1020, May/Jun. 2010.
- [9] M. Marchesoni and C. Vacca, “New DC–DC converter for energy storage system interfacing in fuel cell energy
- [10] **High Step-Up Converter for closed loop controller with Three-Winding Coupled Inductor for Renewable Energy Sources** source applications,” IEEE Trans. Power. Electron., vol. 22, no. 1, pp. 301–308, Jan. 2007.
- [10] G.-J. Su and L. Tang, “A reduced-part, triple-voltage DC-DC converter for EV/HEV power management,” IEEE Trans. Power Electron., vol. 24, no. 10, pp. 2406–2410, Oct. 2009.
- [11] S. M. Dwari and L. Parsa, “A novel high efficiency high power interleaved coupled-inductor boost DC–DC converter for hybrid and fuel cell electric vehicle,” in Proc. IEEE Veh. Power Propulsion Conf., Sep. 2007, pp. 399–404.
- [12] P. Xuwei and A. K. Rathore, “Novel interleaved bidirectional snubber less soft-switching current-fed full-bridge voltage doubler for fuel cell vehicles,” IEEE Trans. Power Electron., vol. 28, no. 12, pp. 5535–5546, Dec. 2013.
- [13] A. K. Rathore and U. R. Prasanna, “Analysis, design, and experimental results of novel snubber less bidirectional naturally clamped ZCS/ZVS current-fed half-bridge dc/dc converter for fuel cell vehicles,” IEEE Trans. Ind. Electron., vol. 60, no. 10, pp. 4482–4491, Oct. 2013.
- [14] O. Hegazy, J. Van Mierlo, and P. Lataire, “Analysis, modeling, and implementation of a multi device interleaved dc/dc converter for fuel cell hybrid electric vehicles,” IEEE Trans. Power Electron., vol. 27, no. 11, pp. 4445–4458, Nov. 2012.